

1 **CriMCE: A method to introduce and isolate precise marker-less edits via**  
2 **CRISPR-mediated cassette exchange**

3  
4 Ioanna Morianou<sup>1</sup>, Andrea Crisanti<sup>1,2</sup>, Tony Nolan<sup>3</sup>, Andrew M. Hammond<sup>1,4,5\*</sup>

5  
6 \*Corresponding author

7  
8  
9 Author Affiliations:

10  
11 <sup>1</sup>Department of Life Sciences, Imperial College London, London, UK

12 <sup>2</sup>Department of Molecular Medicine, University of Padova, Padua, Italy

13 <sup>3</sup>Department of Vector Biology, Liverpool School of Tropical Medicine, Liverpool, UK

14 <sup>4</sup>Department of Molecular Microbiology and Immunology, Johns Hopkins Bloomberg School of Public Health,  
15 Johns Hopkins University, Baltimore, MD, USA

16 <sup>5</sup>Biocentis, Ltd., London, UK

17  
18  
19  
20 Running head:

21  
22 CRISPR-based method for marker-less editing

23  
24  
25 Keywords:

26  
27 CRISPR; genome editing; cassette exchange; marker-less edits; gene drive.  
28  
29  
30  
31  
32  
33  
34  
35  
36  
37  
38  
39  
40  
41  
42  
43  
44  
45  
46  
47  
48  
49  
50  
51  
52  
53  
54  
55  
56  
57  
58  
59  
60  
61  
62  
63  
64  
65  
66

67 **Abstract**

68  
69  
70  
71  
72  
73  
74  
75  
76  
77  
78  
79  
80  
81  
82  
83  
84  
85  
86  
87  
88  
89  
90  
91  
92  
93  
94  
95  
96  
97  
98  
99  
100  
101  
102  
103  
104  
105  
106  
107  
108  
109  
110  
111  
112  
113  
114  
115  
116  
117  
118  
119  
120  
121

The introduction of small, unmarked edits to the genome of insects is essential to study the molecular underpinnings of important biological traits, such as resistance to insecticides and genetic control strategies. Advances in CRISPR genome engineering have made this possible, but prohibitively laborious for most laboratories due to low rates of editing and the lack of a selectable marker. To facilitate the generation and isolation of precise marker-less edits we have developed a two-step method based upon CRISPR-mediated cassette exchange (CriMCE) of a marked placeholder for a variant of interest. This strategy can be used to introduce a wider range of potential edits compared to previous approaches whilst consolidating the workflow. We present proof-of-principle that CriMCE is a powerful tool by engineering three SNP variants into the genome of *Anopheles gambiae*, with 5-41x higher rates of editing than homology-directed repair or prime editing.

122 **Introduction**

123  
124 Small genetic changes, such as single nucleotide polymorphisms (SNPs), can give rise to  
125 prominent phenotypes. For example, they are responsible for most genetic diseases in  
126 humans,<sup>1</sup> important agronomic traits in plants,<sup>2</sup> and insecticide resistance in insect vectors of  
127 disease.<sup>3</sup>

128  
129 To study their molecular underpinning, it is essential to engineer small precise edits like  
130 these in the laboratory,<sup>4</sup> whilst excluding any transformation markers or gene editing debris  
131 that could interfere with the observed phenotype. The introduction of such marker-less edits  
132 has been facilitated by the discovery and expansion of CRISPR (clustered regularly  
133 interspersed short palindromic repeats) technologies.

134  
135 In its most common form, CRISPR genome editing comprises a Cas endonuclease, able to  
136 catalyse a DNA double-stranded break (DSB); and a guide RNA (gRNA) that directs the Cas  
137 protein to its target sequence.<sup>5</sup> Simple and complex edits can be introduced with precision at  
138 a CRISPR-induced break by presenting a modified DNA template for homology directed  
139 repair (HDR). Recently developed base editing and prime editing methods are less versatile  
140 but work independently of the HDR pathway and can raise the efficiency of editing in species  
141 where HDR is naturally low.<sup>6-10</sup> Base editing can induce transition point mutations through a  
142 Cas-deaminase fusion, whilst prime editing can introduce any point mutation or small indel  
143 by employing a Cas-reverse transcriptase fusion and a prime editing gRNA (pegRNA) that  
144 functions as a template for repair.<sup>11</sup> Neither have been widely tested in insects, however  
145 initial trials in *Drosophila* suggest that prime editing is no more efficient than HDR,<sup>12</sup> whilst  
146 base editing is effective but inherently imprecise.<sup>13</sup>

147  
148 In insects, independent of the chosen technology, engineering small marker-less edits  
149 remains inefficient, with transformation rates rarely exceeding 5%.<sup>12,14,15</sup> The lack of a  
150 molecular marker further hinders the process of identifying and isolating rare transformants,  
151 which becomes prohibitively laborious, relying upon large numbers of single crosses and  
152 molecular identification of variants. Although there has been an expansion in the methods to  
153 engineer marker-less edits, this has not been met with a similar level of expansion in  
154 methods to isolate rare transformants.

155  
156 We devised a two-step method to generate and facilitate the detection and isolation of  
157 precise marker-less edits, based upon CRISPR-mediated cassette exchange (CriMCE) of a  
158 marked placeholder for a variant of interest (**Figure 1A**). CriMCE relies upon the visual  
159 detection of an edit, through the loss of a marker (**Figure 1A**), which serves to enrich the  
160 pool of molecularly queried individuals for rare transformants, to reduce the labour and time  
161 required to isolate them (**Figure 1C**).

162  
163 We demonstrate the value of CriMCE by deliberately introducing three SNP variants into the  
164 genome of the malaria mosquito, *Anopheles gambiae*, at the target site of a synthetic gene  
165 drive in the *doublesex* gene.<sup>16,17</sup> Gene drives are engineered selfish genetic elements that  
166 show promise in controlling disease vector populations,<sup>16,18-20</sup> but are susceptible to resistant  
167 mutations arising at the gene drive target site, in the form of SNPs or small indels.<sup>21-23</sup> For  
168 vector control strategies, including insecticides and gene drive, it is becoming increasingly  
169 important to anticipate the emergence of resistance and pre-emptively design contingency  
170 plans. The SNP variant strains generated in this study will be useful in studying the potential  
171 for resistance to gene drives targeting a highly conserved site on *doublesex* and will inform  
172 implementation strategies.

173  
174 We show that CriMCE is more efficient than methods previously employed to introduce  
175 small, unmarked edits,<sup>12,14,15</sup> whilst retaining versatility that would allow the engineering of  
176 more complex modifications as well (**Figure 1B**).

177 **Materials and Methods**

178

179 Molecular cloning of CRISPR plasmids

180

181 We used Golden Gate cloning to insert a dual gRNA expression cassette into the p174  
182 master vector,<sup>16</sup> to generate CRISPR vectors p174102 and p17404 needed to catalyse  
183 genomic cleavage for the insertion of a placeholder cassette and the variant of interest,  
184 respectively. We first amplified a gRNA scaffold-U6 terminator-U6 promoter sequence, from  
185 plasmid p131 using primers containing *BsaI* sites (underlined), and gRNA sequences  
186 (capitals): *BsaI*-T1-U6-F

187 (gagggctctcatgctGTTTAACACAGGTCAAGCGGggttttagagctagaaatagcaagt) and *BsaI*-T3-U6-R  
188 (gagggctctcaaacCTCTGACGGGTGGTATTGCagcagagagcaactccatttcat), to add *doublesex*  
189 targeting gRNAs onto p174 and *BsaI*-G1-U6-F

190 (gagggctctcatgctGGTTAATTCGAGCTCGCCCGgttttagagctagaaatagcaagt) and *BsaI*-G2-U6-  
191 R (gagggctctcaaacCAACTAGAAATGCAGTGAAACagcagagagcaactccatttcat) to add  
192 placeholder targeting gRNAs. The PCR products were inserted into p174, through  
193 GoldenGate cloning, to create CRISPR vectors p174102 and p17404, containing a  
194 *zpg::hCas9*, a *3xP3::DsRed::SV40* marker and U6-expressed *doublesex*-targeting gRNAs  
195 (T1 and T3) or placeholder-targeting gRNAs (G1 and G3), respectively.

196

197 Molecular cloning of placeholder donor plasmid

198

199 A *3xP3::GFP::SV40* marker cassette was amplified from plasmid pK101,<sup>16</sup> using primers  
200 *Sgsl-3xP3-F* (GGCGCGCCCCACAATGGTTAATTCGAGC) and *Sgsl-SV40-R*  
201 (GGCGCGCCAAGATACATTGATGAGTTTGGAC). Genomic DNA regions ~1.8 kb upstream  
202 and downstream of the *doublesex* intron 4-exon 5 splice junction were amplified using primer  
203 pairs: 4050-KI-Gib1

204 (GCTCGAATTAACCATTGTGGACCGGTCTTGTGTTTAGCAGGCAGGGGA) with 4050-KI-  
205 Gib31 (TCCAACTCATCAATGTATCTTGGCGCGCCATAAATGAATGGAAAGGTAAGGC),  
206 and 4050-KI-Gib32

207 (GAGCTCGAATTAACCATTGTGGGGCGCGCCGTATCTTTGTATGTGGGTGTGTG) with  
208 4050-KI-Gib4

209 (TCCACCTCACCCATGGGACCCACGCGTGGTGGCGGGTCACCGAGATGTTC), to make up  
210 the right and left homology arms, respectively, of the donor plasmid. To generate the  
211 placeholder donor plasmid pHolder-dsx the three PCR products were combined with a  
212 digested vector backbone containing a *3xP3::DsRed::SV40* marker cassette in a four-  
213 fragment Gibson assembly, so that the *dsx* homology arms flank the GFP placeholder  
214 cassette.

215

216 Molecular cloning of variant donor plasmids

217

218 An intermediate plasmid (pVar-dsx) was Gibson assembled to contain the same vector  
219 backbone and homology arms as pHolder, and a sequence containing *BsaI* cloning sites,  
220 flanking the region of interest of an otherwise intact exon 5 (**Supplementary Figure 1A-C**).

221 This allowed the Golden Gate cloning of annealed oligos containing three different  
222 *doublesex* exon 5 variants: a G→A SNP (GTTTAACACAGGTCAAGCAGTGGT,  
223 chromosome 2, position 47,997,665), a C→T SNP (GTTTAACACAGGTCAAGTGGTGGT,  
224 chromosome 2, position 47,997,666) and a G→T SNP (GTTTAACACAGGTCAATCGGTGG,  
225 chromosome 2, position 47,997,667). The same plasmid, pVar-dsx, can be used to clone  
226 and study more variants at the same target site in the future.

227

228 Embryo microinjections

229

230 *Anopheles gambiae* G3 strain mosquitoes were reared at 26±2°C and 65±10% relative  
231 humidity and blood-fed on cow blood using Hemotek membrane feeders.<sup>18</sup> Microinjections

232 were performed on freshly laid embryos as previously described.<sup>24</sup> Each microinjected  
233 plasmid was present in solution at 300 ng/μl.

234

235 To generate the placeholder strain, wild-type embryos were microinjected with the p174102  
236 CRISPR plasmid and pHolder donor plasmid (**Supplementary Figure 1D-E**). In  
237 transformants, this caused the excision of the coding sequence (CDS) of the female-specific  
238 exon 5 of the *doublesex* gene and its replacement with a GFP marker cassette. All  
239 microinjection survivors (G0) were crossed to wild-type mosquitoes and positive  
240 transformants (G1) were identified through fluorescence microscopy, as GFP+.

241

242 To generate the SNP variant strains, placeholder homozygote males were crossed to  
243 placeholder heterozygote females, distinguished using the COPAS fluorescence-based  
244 larval sorter.<sup>25</sup> Their progeny was microinjected with the p174104 CRISPR plasmid and each  
245 of the variant donor plasmids (pVar-dsxGA, pVar-dsxCT, pVar-dsxGT) (**Supplementary**  
246 **Figure 1D-E**). In successful transformants, this caused the CRISPR-mediated cassette  
247 exchange of the marked placeholder for the *doublesex* exon 5 variants. Injected survivors  
248 (G0) were distinguished from non-injected survivors (G0), as they exhibited red fluorescence  
249 in their posterior, due to successful injection of the p174104 CRISPR plasmid, containing a  
250 DsRed cassette in its backbone, which acted as a co-injection marker (**Supplementary**  
251 **Figure 1D-E**). All injected survivors (G0) were crossed to wild-type and females were  
252 deposited to lay eggs individually. A decreased inheritance of the marked placeholder  
253 (GFP+) in G1 progeny indicated CRISPR-mediated cassette exchange of the placeholder for  
254 the variant sequence (**Figure 2**).

255

#### 256 Molecular genotyping

257

258 Genomic DNA was extracted from queried individuals after they gave offspring, in single  
259 samples, amplified using primers dsx-exon5-R4 (AACTTATCGGCATCAGTTGCG) and dsx-  
260 intron4-F1 (GTGAATTCCGTCAGCCAGCA) and sequenced using the dsx-exon5-R2 primer  
261 (TGAATTCGTTTCACCAAACACAC), to decipher their genotype.

262

#### 263 Analysis

264

265 Figures were designed on Biorender (full licence) and Adobe Illustrator and graphs were  
266 plotted and statistically analysed on Graphpad Prism 9.

267

268

269

## 270 **Results**

271

272 We tested the efficiency of CriMCE and demonstrated proof of principle by using it to  
273 engineer and isolate mutations that potentially confer resistance to a gene drive, previously  
274 developed against the *doublesex* (*dsx*) gene in the malaria mosquito, *Anopheles gambiae*.<sup>16</sup>

275

276 First, we generated a placeholder strain by inserting a GFP cassette in place of the entire  
277 female-specific exon (exon 5) of *dsx* via CRISPR-mediated HDR (**Figure 2A**). This strain  
278 was isolated based on GFP fluorescence, and displayed an intersex phenotype in  
279 homozygous females, consistent with the null mutation.<sup>16</sup>

280

281 We then performed CRISPR-mediated cassette exchange (CriMCE) of the placeholder for  
282 the marker-less SNP of interest (G→A, C→T or G→T), by injecting placeholder  
283 homozygotes and heterozygotes with a plasmid expressing Cas9 and gRNAs targeted to the  
284 placeholder, and a template for repair encoding the variant of interest (**Supplementary**  
285 **Figure 1D-E, 3B**). To maximise the recovery of editing events, we selected only the fraction  
286 of injected mosquitoes that showed transient RFP fluorescence as clear evidence of having

287 taken up the CRISPR expression vector (**Supplementary Figure 1D-E**) and mated these to  
288 wild-type (**Figure 3**).  
289

290 CriMCE-induced editing was evidenced by loss of GFP (<100% GFP inheritance) among the  
291 offspring of placeholder homozygotes, or by significant deviation below the Mendelian  
292 expectation of 50% GFP inheritance among the offspring of placeholder heterozygotes  
293 (**Figure 3**). We saw rates of precise editing up to 39% for the G→A SNP (evidenced by 61%  
294 GFP inheritance in the offspring of placeholder homozygotes) (**Figure 3A**), up to 100% for  
295 the C→T SNP, and up to 92% for the G→T SNP variant (evidenced by 0% and 4% GFP  
296 inheritance in the offspring of placeholder heterozygotes, respectively) (**Figure 3B**).  
297 Incorporation of the SNPs of interest was confirmed by Sanger sequencing (**Supplementary**  
298 **Figure 2**). Notably, we did not detect any end-joining (EJ) events (N=55). Owing to the high  
299 rates of editing by CriMCE, G1 transformants that showed low levels of GFP inheritance can  
300 be immediately crossed to the placeholder strain that will act as a balancer, for rapid  
301 characterisation of each marker-less edit.  
302

303 In two G1 clutches with altered GFP inheritance we also detected variant donor plasmid  
304 integration, evidenced by RFP at 2% and 18% amongst GFP negatives (with a median of  
305 0% taken across all modified clutches) (**Supplementary Figure 1**). These were not  
306 considered as true transformants in our analysis (**Table 1, Figure 4**).  
307

308 To compare our method to previously developed strategies employing HDR and prime  
309 editing to introduce and isolate marker-less edits,<sup>12,14,15</sup> we calculated three measures of  
310 transformation efficiency: the percentage of G0 founders that gave G1 transformants, the G1  
311 transformant to G0 injected survivor ratio, and the G1 transformant percentage out of all G1  
312 screened (**Table 1**). If the G1 transformant to G0 injected survivor ratio is high, then a high  
313 number of transformants can be obtained from a smaller number of injected survivors; whilst  
314 having a high percentage of G1 transformants out of total G1 screened, implies a reduced  
315 requirement for screening, whether this is done visually, like in the present study (less  
316 laborious), or by PCR and sequencing analysis, like in previous studies (more laborious). As  
317 a reference, we also show the efficiency of locus-specific marked transgene insertion  
318 through RMCE and HDR (**Table 1**).  
319

320 In total, we detected visible editing in the progeny of 7/18 (38.9%) G0 micro-injected  
321 individuals with the G→A construct, 3/8 (37.5%) G0 micro-injected individuals with the C→T  
322 construct, and 4/9 (44.4%) G0 micro-injected individuals with the G→T construct (**Figure 3,**  
323 **Table 1**).  
324

325 CriMCE offers a marked improvement in transformation efficiency when compared to other  
326 approaches employed to introduce marker-less edits (**Figure 4**). Specifically, CriMCE shows  
327 a mean G1 transformant to G0 injected survivor ratio of 5.76 ( $\pm 2.37$  s.d.), compared to 0.14  
328 ( $\pm 0.10$  s.d.) for direct HDR (Welch's t-test  $p=0.031$ ) and 1.06 ( $\pm 0.83$  s.d.) for prime editing;  
329 and a mean G1 transformant per G1 screened percentage of 10.5% ( $\pm 6.0\%$  s.d.), compared  
330 to 1.0% ( $\pm 0.5\%$  s.d.) for direct HDR and 1.4% ( $\pm 1.1\%$  s.d.) for prime editing (Welch's t-test  
331  $p=0.058$ ) (**Figure 4**).  
332  
333

## 334 Discussion

335

336 To address the difficulty in engineering and isolating marker-less edits in insects, we have  
337 developed a strategy based upon CRISPR-mediated cassette exchange (CriMCE) of a  
338 marked placeholder for a variant of interest, allowing visual detection of transformation.  
339

340 Unlike other two-step methods for marked cassette exchange or removal, like recombinase-  
341 mediated cassette exchange (RMCE) and Cre-Lox recombination, CriMCE relies upon HDR.  
342 This allows for comparatively high efficiency (when compared to RMCE) (**Table 1**), and  
343 uniquely traceless editing such that any phenotypic change can be attributed to the intended  
344 edit rather than ruminant attachment sites (**Figure 1**). Co-conversion of a target locus  
345 together with a gene that produces a visual phenotype is another HDR-based strategy that  
346 has been used to improve isolation of marker-less edits.<sup>26</sup> This filters individuals showing  
347 CRISPR activity, however it does not distinguish HDR events that incorporate the desired  
348 edit, from EJ events carrying unwanted indels.<sup>26</sup>

349  
350 Increasing the relative frequency of HDR over error-prone EJ repair remains difficult. Our  
351 strategy leverages loss of a marked placeholder (GFP+) to indicate precise editing by HDR.  
352 By targeting CRISPR to non-coding regions of the placeholder, undesirable EJ events are  
353 screened out as they are unlikely to affect GFP expression. Furthermore, we express Cas9  
354 under the control of *zpg* regulatory elements that are spatiotemporally restricted to enhance  
355 HDR.<sup>27</sup> Indeed, no EJ mutations were detected in GFP- negative transformants. This  
356 focuses molecular identification by PCR and sequencing on individuals carrying the desired  
357 edit, therefore reducing the rearing effort required to enrich the frequency of marker-less  
358 variants (**Supplementary Figure 3**).

359  
360 Somewhat surprisingly, rates of HDR-induced editing are relatively high when marked  
361 mutations are introduced (**Table 1**),<sup>23,28-30</sup> but drop substantially when SNPs are directly  
362 inserted into a wild-type genomic locus, in *Aedes aegypti* and *An. gambiae* (**Table 1, Figure**  
363 **4**).<sup>14,15</sup> Using CriMCE in *An. gambiae* we achieved high rates of HDR editing consistent with  
364 those for marked edit insertion in *An. gambiae* and *D. melanogaster* (**Table 1, Figure 4**).<sup>28,29</sup>  
365 In both cases, repair templates differ significantly from their target regions: transgenes  
366 introduced via HDR do not resemble their genomic target, while in the present study the  
367 wild-type target is replaced by a placeholder, which serves to differentiate it from the desired  
368 edit (**Figure 2**). Conversely, when direct HDR is used to induce small marker-less edits the  
369 repair template is almost identical to that of the wild-type target. It is still unclear why  
370 sequence dissimilarity between the exogenous repair template and its target should boost  
371 the efficiency of editing, but perhaps it functions to shift repair away from using the  
372 unmodified homologous chromosome as a template. Non-plasmid-based templates could  
373 also be used in a CriMCE strategy, such as single-stranded oligodeoxynucleotide (ssODN)  
374 that are simpler to produce and might further increase the rates of editing.<sup>31</sup>

375  
376 CriMCE might be less efficient in species with inherently low rates of HDR, such as *An.*  
377 *stephensi* (**Table 1**),<sup>20,23</sup> and alternatives not reliant upon HDR, like base and prime editing,<sup>11</sup>  
378 have not yet been tested in non-model insects. In these species, CriMCE can be optimised  
379 by injecting placeholder homozygotes, so that rare events are distinguished by visual  
380 inspection alone (**Figure 3A**).

381  
382 The CriMCE method can also mitigate against the risk of using previously untested and  
383 potentially inefficient gRNAs/pegRNAs that would otherwise expend undue effort on genetic  
384 crosses and molecular genotyping. Generating a marked placeholder prior to precise editing  
385 ensures that rare transgenesis using novel gRNA/pegRNAs is easily identifiable by a  
386 fluorescent marker. Previously tested guides can then be used to target the placeholder,  
387 inducing CriMCE. In this study we validate the use of two gRNAs that target a universal  
388 placeholder which is designed to function across insect species.

389  
390 CriMCE is particularly powerful for experiments aimed at introducing a range of modifications  
391 to a single locus of interest, as a single placeholder strain can be exchanged for any number  
392 of variants. Indeed, a similar approach, based upon exchange of a marked allele for  
393 engineering of *kdr* pyrethroid resistance mutations was employed in *Drosophila*,<sup>32</sup> and could  
394 be further extended to incorporate newly discovered insecticide resistant SNPs.<sup>33</sup>

395  
396 Moreover, CriMCE allows for complex mutations that are not possible using prime editing  
397 since the entire region ablated by the placeholder can be replaced with a region bearing any  
398 number of desired edits. This strategy, which we term allelic exchange (**Figure 1C**), could  
399 allow multiple linked SNPs to be introduced across a wide genetic locus. This would be  
400 useful in assessing how various resistant SNPs interact with each other to produce complex  
401 insecticide resistance phenotypes.<sup>4</sup> Other complex edits are also possible such as the  
402 introduction, modification or deletion of introns and splice site, or complete codon scrambling  
403 by which a coding sequence is modified without affecting the encoded amino acid sequence  
404 (**Figure 1C**). The latter strategy could serve to engineer synthetic alleles that are resistant to  
405 gene drive elements as a mechanism for gene drive recall.<sup>34</sup>  
406

407 Finally, we describe how CriMCE can be used to target haploinsufficient genes, which by  
408 their nature, would be unable to tolerate a disruption from the placeholder, even if the  
409 desired edit is anticipated to be viable. In this case, integrating the placeholder within  
410 proximal intronic or neutral regions should permit editing (**Supplementary Figure 4**).  
411

412

## 413 **Conclusions**

414

415 CriMCE is an efficient method to introduce and isolate precise and potentially complex  
416 marker-less edits by exchange of a visually marked intermediate. Our proof-of-principle  
417 experiments in *Anopheles gambiae* suggest that CriMCE is 5-41x more efficient than other  
418 strategies based on HDR or prime editing, whilst enabling an expanded range of potential  
419 edits and consolidating the workflow. In our experience the use of a placeholder strain does  
420 not prolong isolation of the desired edit and can be used as an important control or balancer  
421 in assessing its phenotype. We believe this strategy will be important in linking small genetic  
422 changes with a biologically relevant outcome across a range of insect species, with  
423 particular applications in the study of resistance to insecticides and gene drive technologies.  
424

425

426

427

## 427 **Acknowledgements**

428

429 We thank Louise Marston, Matthew Gribble and Molly McGrath for their help towards  
430 generating and maintaining transgenic strains.  
431

432

433

434

## 434 **Author contribution statement**

435

436 The idea was conceived by I.M., A.C. and A.M.H. The experiments were designed by I.M.  
437 with input from T.N. and A.M.H. The experiments, data visualisation and analysis were  
438 performed by I.M. The original draft was written by I.M. and edited by A.M.H. The manuscript  
439 was reviewed by all authors.  
440

441

442

443

## 443 **Conflict of interest statement**

444

445 A.C. and A.M.H. are founders of Biocentis, Ltd. A.C., T.N. and A.M.H. have an equity  
446 interest in Biocentis, Ltd. I.M. declares no conflict of interest.  
447

448

449



450  
451  
452  
453  
454  
455  
456  
457  
458  
459  
460  
461  
462  
463  
464  
465  
466  
467  
468  
469  
470  
471  
472  
473  
474  
475  
476  
477  
478  
479  
480  
481  
482  
483  
484  
485  
486  
487  
488  
489  
490  
491  
492  
493  
494  
495  
496  
497  
498  
499  
500  
501  
502  
503

## Funding statement

This work was supported by funding from a Medical Research Council (MRC) Doctoral Training Partnership (DTP) and grants from the Bill & Melinda Gates Foundation (BMGF). Funders had no role in study design, data collection and analysis, decision to publish, or preparation of the manuscript.

## References

1. Wang Z and Moutl J. SNPs, Protein Structure, and Disease. *Human Mutation* 2001;17(4):263–270; doi: 10.1002/humu.22.
2. Mishra R, Joshi RK and Zhao K. Base Editing in Crops: Current Advances, Limitations and Future Implications. *Plant Biotechnology Journal* 2020;18(1):20–31; doi: 10.1111/pbi.13225.
3. Hemingway J and Ranson H. Insecticide Resistance in Insect Vectors of Human Disease. *Annu Rev Entomol* 2000;45:371–391; doi: 10.1146/annurev.ento.45.1.371.
4. Samantsidis GR, Panteleri R, Denecke S, et al. 'What I Cannot Create, I Do Not Understand': Functionally Validated Synergism of Metabolic and Target Site Insecticide Resistance. *Proceedings of the Royal Society B: Biological Sciences* 2020;287(1927); doi: 10.1098/rspb.2020.0838.
5. Hsu PD, Lander ES and Zhang F. Development and Applications of CRISPR-Cas9 for Genome Engineering. *Cell* 2014;157(6):1262–1278; doi: 10.1016/j.cell.2014.05.010.
6. Petri K, Zhang W, Ma J, et al. CRISPR Prime Editing with Ribonucleoprotein Complexes in Zebrafish and Primary Human Cells. *Nature Biotechnology* 2021;1–5; doi: 10.1038/s41587-021-00901-y.
7. Lin Q, Jin S, Zong Y, et al. High-Efficiency Prime Editing with Optimized, Paired PegRNAs in Plants. *Nature Biotechnology* 2021 39:8 2021;39(8):923–927; doi: 10.1038/s41587-021-00868-w.
8. Villiger L, Grisch-Chan HM, Lindsay H, et al. Treatment of a Metabolic Liver Disease by in Vivo Genome Base Editing in Adult Mice. *Nature Medicine* 2018 24:10 2018;24(10):1519–1525; doi: 10.1038/s41591-018-0209-1.
9. Gao P, Lyu Q, Ghanam AR, et al. Prime Editing in Mice Reveals the Essentiality of a Single Base in Driving Tissue-Specific Gene Expression. *Genome Biology* 2021;22(1):1–21; doi: 10.1186/s13059-021-02304-3.
10. Li C, Zong Y, Wang Y, et al. Expanded Base Editing in Rice and Wheat Using a Cas9-Adenosine Deaminase Fusion. *Genome Biology* 2018;19(1):1–9; doi: 10.1186/S13059-018-1443-z.
11. Anzalone A v., Koblan LW and Liu DR. Genome Editing with CRISPR–Cas Nucleases, Base Editors, Transposases and Prime Editors. *Nature Biotechnology* 2020 38:7 2020;38(7):824–844; doi: 10.1038/s41587-020-0561-9.
12. Bosch JA, Birchak G and Perrimon N. Precise Genome Engineering in *Drosophila* Using Prime Editing. *Proc Natl Acad Sci U S A* 2020;118(1); doi: 10.1073/pnas.2021996118.
13. Marr E and Potter CJ. Base Editing of Somatic Cells Using CRISPR-Cas9 in *Drosophila*. *CRISPR Journal* 2021;4(6):836–845; doi: 10.1089/crispr.2021.0062
14. Grigoraki L, Cowlshaw R, Nolan T, et al. CRISPR/Cas9 Modified An. Gambiae Carrying Kdr Mutation L1014F Functionally Validate Its Contribution in Insecticide Resistance and Combined Effect with Metabolic Enzymes. *PLOS Genetics* 2021;17(7):e1009556; doi: 10.1371/journal.pgen.1009556.
15. Kistler KE, Vosshall LB and Matthews BJ. Genome Engineering with CRISPR-Cas9 in the Mosquito *Aedes Aegypti*. *Cell Rep* 2015;11(1):51–60; doi: 10.1016/j.celrep.2015.03.009.

- 504 16. Kyrou K, Hammond AM, Galizi R, et al. A CRISPR–Cas9 Gene Drive Targeting  
505 Doublesex Causes Complete Population Suppression in Caged Anopheles Gambiae  
506 Mosquitoes. *Nature Biotechnology* 2018; doi: 10.1038/nbt.4245.
- 507 17. Morianou I, Hammond AM, Crisanti A, et al. In Preparation. London; 2022.
- 508 18. Hammond A, Pollegioni P, Persampieri T, et al. Gene-Drive Suppression of Mosquito  
509 Populations in Large Cages as a Bridge between Lab and Field. *Nature*  
510 *Communications* 2021 12:1 2021;12(1):1–9; doi: 10.1038/s41467-021-24790-6.
- 511 19. Carballar-Lejarazú R, Ogaugwu C, Tushar T, et al. Next-Generation Gene Drive for  
512 Population Modification of the Malaria Vector Mosquito, *Anopheles Gambiae*. *Proc*  
513 *Natl Acad Sci U S A* 2020;117(37):22805–22814; doi: 10.1073/pnas.2010214117.
- 514 20. Adolfi A, Gantz VM, Jasinskiene N, et al. Efficient Population Modification Gene-Drive  
515 Rescue System in the Malaria Mosquito *Anopheles Stephensi*. *Nature*  
516 *Communications* 2020 11:1 2020;11(1):1–13; doi: 10.1038/s41467-020-19426-0.
- 517 21. Hammond AM, Kyrou K, Bruttini M, et al. The Creation and Selection of Mutations  
518 Resistant to a Gene Drive over Multiple Generations in the Malaria Mosquito. *PLoS*  
519 *Genetics* 2017; doi: 10.1371/journal.pgen.1007039.
- 520 22. Carrami EM, Eckermann KN, Ahmed HMM, et al. Consequences of Resistance  
521 Evolution in a Cas9-Based Sex Conversion-Suppression Gene Drive for Insect Pest  
522 Management. *Proc Natl Acad Sci U S A* 2018;115(24):6189–6194; doi:  
523 10.1073/pnas.1713825115.
- 524 23. Gantz VM, Jasinskiene N, Tatarenkova O, et al. Highly Efficient Cas9-Mediated Gene  
525 Drive for Population Modification of the Malaria Vector Mosquito *Anopheles*  
526 *Stephensi*. *Proc Natl Acad Sci U S A* 2015;112(49):E6736–E6743; doi:  
527 10.1073/pnas.1521077112.
- 528 24. Fuchs S, Nolan T and Crisanti A. Mosquito Transgenic Technologies to Reduce  
529 *Plasmodium* Transmission. *Methods Mol Biol* 2013;923:601–622; doi: 10.1007/978-1-  
530 62703-026-7\_41.
- 531 25. Marois E, Scali C, Soichot J, et al. High-Throughput Sorting of Mosquito Larvae for  
532 Laboratory Studies and for Future Vector Control Interventions. *Malaria Journal* 2012;  
533 doi: 10.1186/1475-2875-11-302.
- 534 26. Tianfang Ge D, Tipping C, Brodsky MH, et al. Rapid Screening for CRISPR-Directed  
535 Editing of the *Drosophila* Genome Using White Coconversion. *G3: Genes, Genomes,*  
536 *Genetics* 2016;6(10):3197–3206; doi: 10.1534/G3.116.032557.
- 537 27. Hammond A, Karlsson X, Morianou I, et al. Regulating the Expression of Gene Drives  
538 Is Key to Increasing Their Invasive Potential and the Mitigation of Resistance. *PLOS*  
539 *Genetics* 2021;17(1):e1009321; doi: 10.1371/journal.pgen.1009321.
- 540 28. Hammond A, Galizi R, Kyrou K, et al. A CRISPR-Cas9 Gene Drive System Targeting  
541 Female Reproduction in the Malaria Mosquito Vector *Anopheles Gambiae*. *Nature*  
542 *Biotechnology* 2016; doi: 10.1038/nbt.3439.
- 543 29. Gratz SJ, Ukken FP, Rubinstein CD, et al. Highly Specific and Efficient  
544 CRISPR/Cas9-Catalyzed Homology-Directed Repair in *Drosophila*. *Genetics*  
545 2014;196(4):961–971; doi: 10.1534/genetics.113.160713.
- 546 30. Ang JX de, Nevard K, Ireland R, et al. Considerations for Homology-Based DNA  
547 Repair in Mosquitoes: Impact of Sequence Heterology and Donor Template Source.  
548 *PLOS Genetics* 2022;18(2):e1010060; doi: 10.1371/journal.pgen.1010060.
- 549 31. Levi T, Sloutskin A, Kalifa R, et al. Efficient in Vivo Introduction of Point Mutations  
550 Using SsODN and a Co-CRISPR Approach. *Biological Procedures Online*  
551 2020;22(1):1–12; doi: 10.1186/S12575-020-00123-7.
- 552 32. Kaduskar B, Kushwah RBS, Auradkar A, et al. Reversing Insecticide Resistance with  
553 Allelic-Drive in *Drosophila Melanogaster*. *Nature Communications* 2022 13:1  
554 2022;13(1):1–8; doi: 10.1038/s41467-021-27654-1.
- 555 33. Clarkson CS, Miles A, Harding NJ, et al. The Genetic Architecture of Target-Site  
556 Resistance to Pyrethroid Insecticides in the African Malaria Vectors *Anopheles*  
557 *Gambiae* and *Anopheles Coluzzii*. *Molecular Ecology* 2021;30(21):5303–5317; doi:  
558 10.1111/mec.15845.

- 559 34. Vella MR, Gunning CE, Lloyd AL, et al. Evaluating Strategies for Reversing CRISPR-  
560 Cas9 Gene Drives. *Scientific Reports* 2017 7:1 2017;7(1):1–8; doi: 10.1038/s41598-  
561 017-10633-2.  
562

**Figure 1. CRISPR-mediated cassette exchange (CriMCE) is a two-step method for engineering the detection and isolation of marker-less edits via CRISPR-mediated homology-directed repair. (A)** Step 1: To generate a marked placeholder strain, the region of interest (gene B) is replaced by a marker (GFP, green). Step 2: The marker is replaced by the native sequence containing the variant of interest (orange), through CRISPR-mediated cassette exchange (CriMCE), to obtain a marker-less strain carrying the variant. **(B)** Examples of the types of simple and complex genetic modifications that can be obtained using CriMCE. **(C)** Comparison of CriMCE to other methods used to make precise genomic edits, including recombinase mediated cassette exchange (RMCE), direct homology-directed repair (HDR) of a wild-type sequence and base or prime editing.

**Figure 2. CriMCE relies upon the generation of a marked placeholder strain, and the subsequent exchange of the placeholder for the variant of interest through CRISPR-mediated HDR. (A)** To generate the marked placeholder strain, the entirety of the exon 5 coding sequence (CDS) was removed via two CRISPR-mediated double-stranded breaks (DSBs) and replaced with a *3xP3::GFP::SV40* marker cassette (green) from a donor plasmid that served as a template for HDR. **(B)** To generate a strain carrying the variant of choice ( $G \rightarrow A$ ,  $C \rightarrow T$  or  $G \rightarrow T$  SNPs at exon 5) the marker cassette was removed via two CRISPR-mediated cleavages and exchanged for the exon 5 CDS containing the variant of interest (orange) from a donor plasmid, through HDR.

**Figure 3. The introduction of a marker-less variant using CriMCE is evidenced by reduced rates of marker inheritance in the progeny of microinjected individuals of the placeholder strain.** Marked placeholder male homozygotes **(A)** and heterozygotes of both sexes **(B)**, were microinjected with a CRISPR helper plasmid and a variant donor plasmid to facilitate CriMCE of the placeholder for one of the variants of interest ( $G \rightarrow A$ ,  $C \rightarrow T$ ,  $G \rightarrow T$ ). G0 parent injected mosquitoes (green) were individually crossed to wild-type (grey) and their G1 progeny screened for GFP fluorescence. Successful introduction of each marker-less variant via CriMCE, was evidenced by a marker frequency of less than 100% in the progeny of placeholder homozygotes, and a marker frequency of less than 50% in the progeny of placeholder heterozygotes (orange). Lack of modification was evidenced by a marker frequency equal to 100% in the progeny of placeholder homozygotes and a marker frequency normally distributed around 50% in the progeny of placeholder heterozygotes (green).

**Figure 4. Comparison of CriMCE to different transgenesis methods for the introduction of small precise marker-less edits.** Welch's t-test p-values of statistical comparisons between CriMCE and prime editing are shown on top of each graph. HDR could not be statistically compared due to its small sample size.

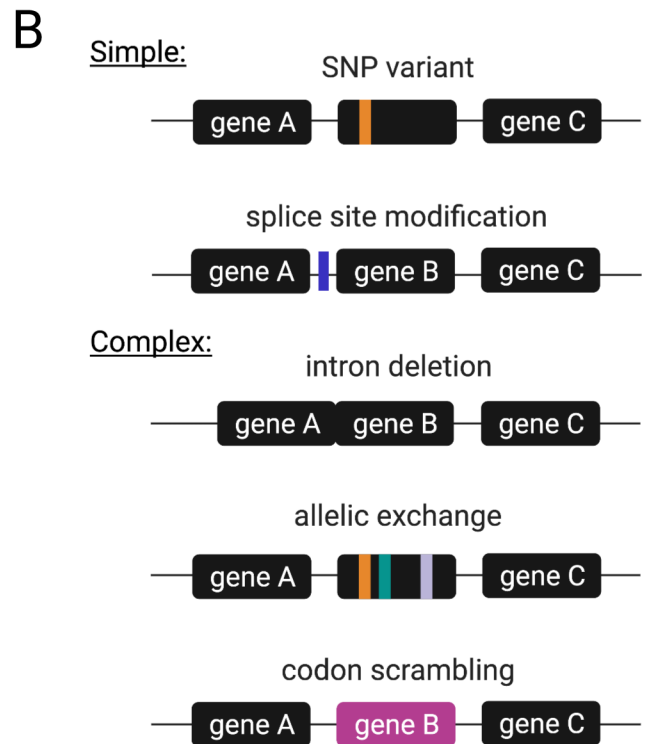
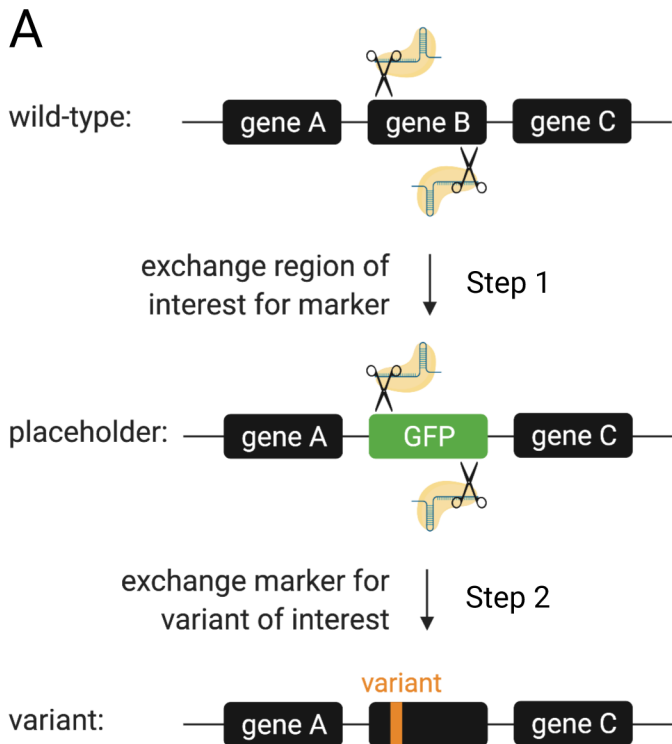
**Supplementary Figure 1. A cloning strategy to create variant donor plasmids and graphical representation of all microinjected plasmids required to facilitate CriMCE.**

**(A)** The donor plasmid precursor contains *Bsal* sites (turquoise) flanked by homology arms complementary to the regions upstream and downstream of the target locus. Through Golden Gate cloning, any variant of interest (orange) can be inserted between the *Bsal* cloning sites, whilst they get removed leaving no molecular trace behind. **(B-C)** To create a variant donor plasmid (using the G→A SNP as an example), *Bsal* recognition sites were introduced upstream and downstream of the 23 bp locus of interest on exon 5. *Bsal* recognition and cleavage sites are distinct, therefore they are placed facing outwards in the donor precursor sequence, to ensure that upon cleavage they get lost, exposing staggered DNA ends on the plasmid precursor. A fragment containing the G→A variant and complementary staggered DNA ends can then be ligated onto the plasmid precursor to make-up the final variant donor plasmid. **(D)** Co-injected plasmids used to generate the marked placeholder strain. **(E)** Co-injected plasmids used to generate the variant strains. **(D-E)** CRISPR plasmids, marked by DsRed (top), express Cas9 under the control of the germline-specific *zpg* regulatory elements, along with two gRNAs under the control of ubiquitous U6 promoters and targeted to the *dsx* exon 5 (**D**, T1 and T3) or the placeholder cassette (**E**, G1 and G2). Donor plasmids for HDR (bottom), were designed to contain either the placeholder GFP cassette (**D**, green) or the *dsx* exon 5 bearing the variant of interest (**E**, orange), flanked by 1.8 kb homology arms complementary to the target region in *doublesex*. Donor plasmid backbones were marked by DsRed.

**Supplementary Figure 2. Molecular validation of successful CriMCE-induced genetic modification through Sanger sequencing.** Sanger sequencing chromatographs from single GFP- mosquitoes. Top: WT, example of an unedited individual. Middle: example of a heterozygous edited individual carrying the SNP variant of interest (G→A, C→T or G→T), evident through a double peak in the chromatograph. Bottom: example of a homozygous edited individual carrying the SNP variant of interest in homozygosis (G→A, C→T or G→T), evident through a single modified peak in the chromatograph. Note that reverse strand sequencing chromatographs are shown.

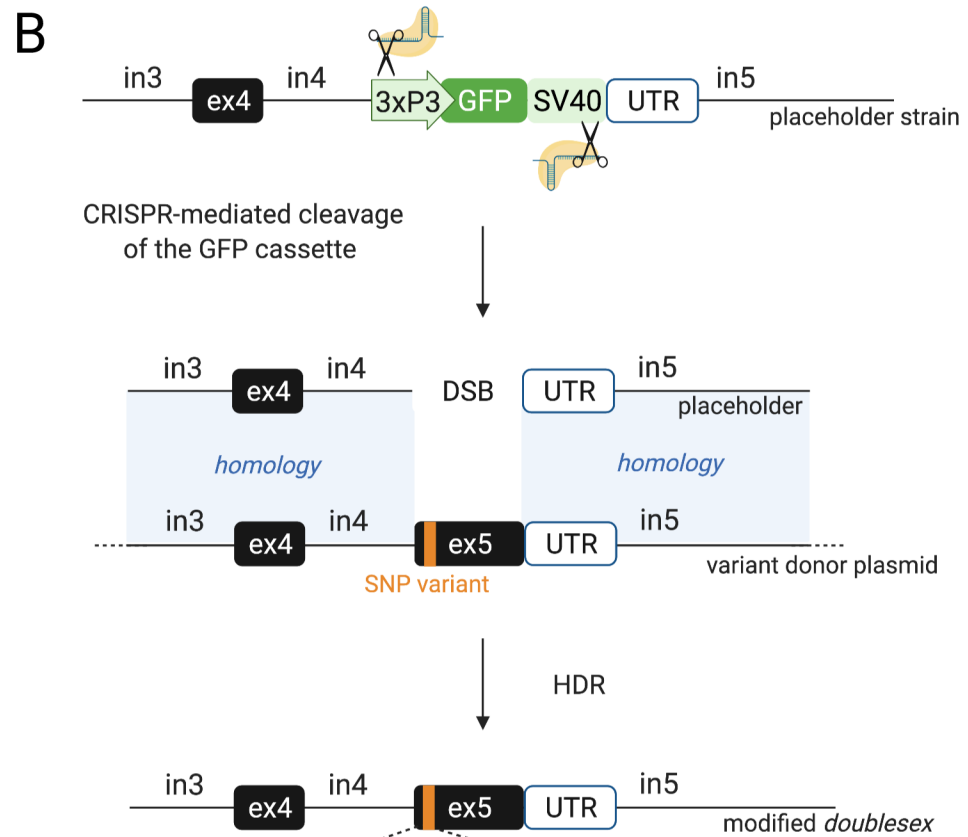
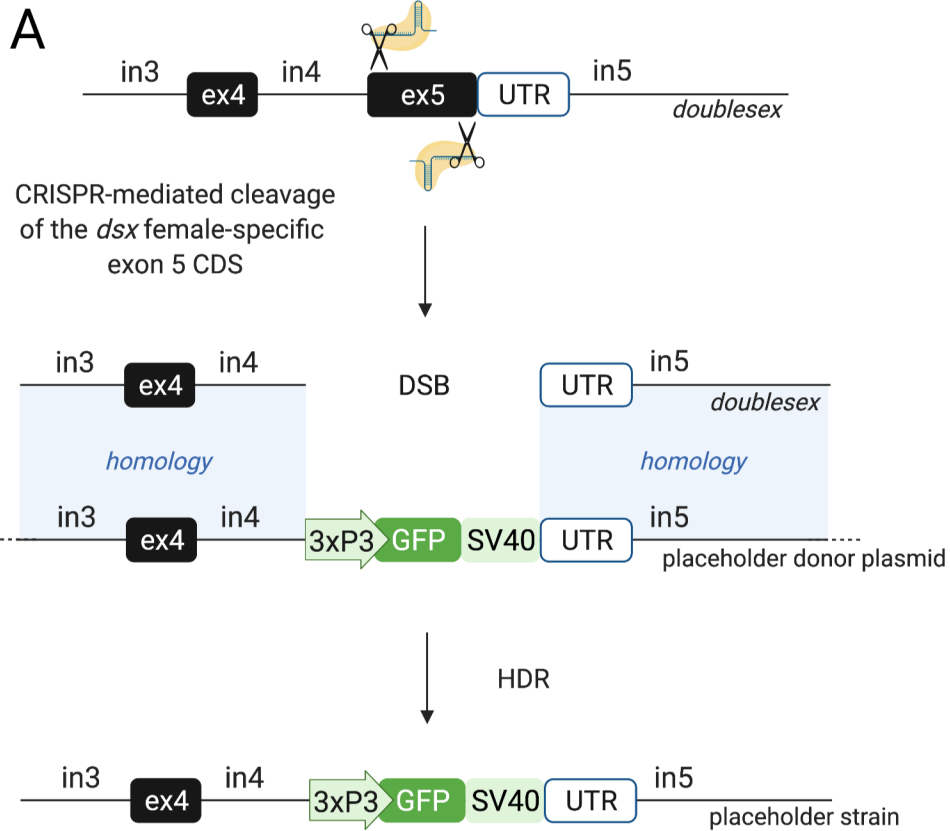
**Supplementary Figure 3. An illustration of the workflow required to isolate a homozygous variant strain when employing CriMCE vs HDR or prime editing for the introduction of precise marker-less edits.** Wild-type mosquitoes are in grey, unmodified mosquitoes in black, placeholder mosquitoes in green, variant heterozygotes in orange, and variant homozygotes in red.

**Supplementary Figure 4. A strategy for introducing precise marker-less edits into haploinsufficient genes using CriMCE.** CriMCE can be adapted to modify haplo-insufficient genes by introducing the marked placeholder into a neutral locus, like an intron, proximal to a target site on a haplo-insufficient exon. **(A)** To generate a marked placeholder strain, a highly variable intronic region, proximal to the haplo-insufficient exon, is cleaved using CRISPR, and a marker cassette (red) is introduced from a donor plasmid, through HDR. **(B)** To generate a strain carrying the variant of choice on the exon the marker cassette is removed via two CRISPR-mediated cleavages: one at the marker cassette and one near the site of interest; and exchanged for an intact sequence containing the variant of choice from a donor plasmid, through HDR. The same strategy could be adopted to allow exclusive microinjection of placeholder homozygotes, provided that the intronic placeholder integration is tolerated in both males and females, to improve CriMCE efficiency in organisms that show inherently low HDR.



**C**

|                    | Visual identification | Scarless strain | Type of modification | Transgenesis steps | Generations to homozygosis (N) | Rearing effort | Generations sequenced |
|--------------------|-----------------------|-----------------|----------------------|--------------------|--------------------------------|----------------|-----------------------|
| CriMCE             | ✓                     | ✓               | Simple & complex     | 2                  | 3                              | medium         | 1-2                   |
| RMCE               | ✓                     | ✗               | Simple & Complex     | 2                  | 3                              | medium         | 1-2                   |
| HDR                | ✗                     | ✓               | Simple & Complex     | 1                  | 4                              | very high      | 3-4                   |
| base/prime editing | ✗                     | ✓               | Simple               | 1                  | 4                              | very high      | 3-4                   |

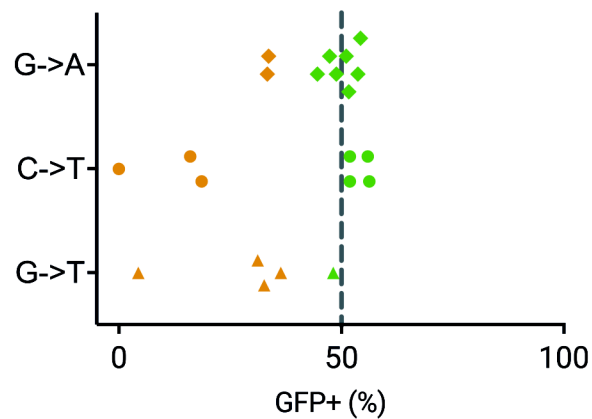
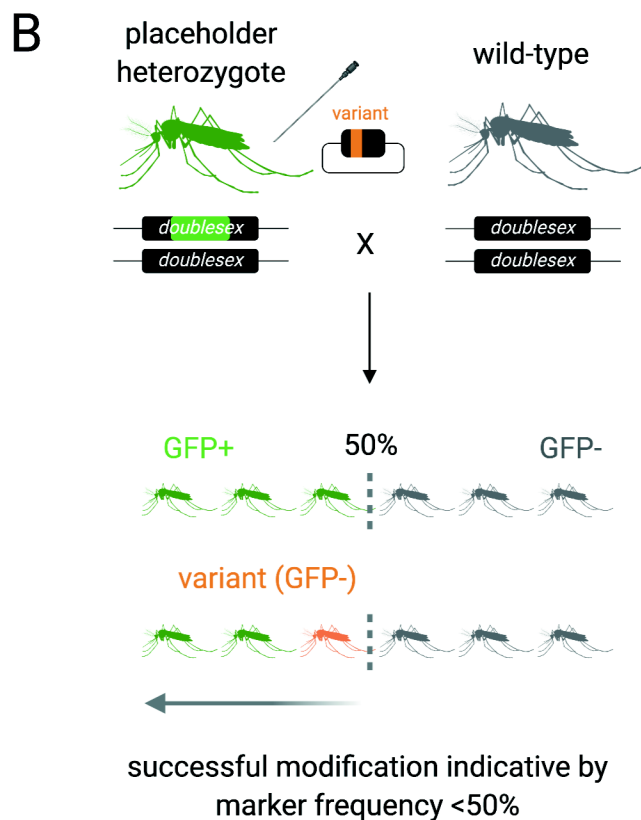
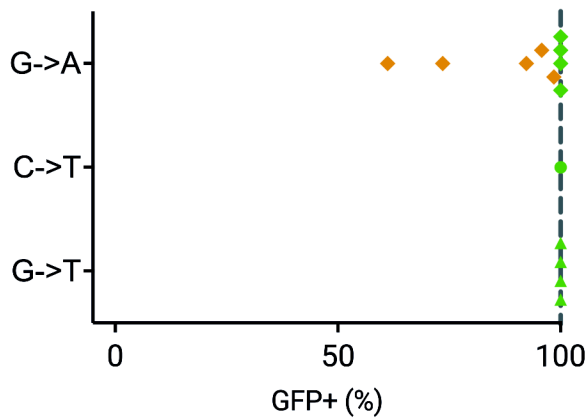
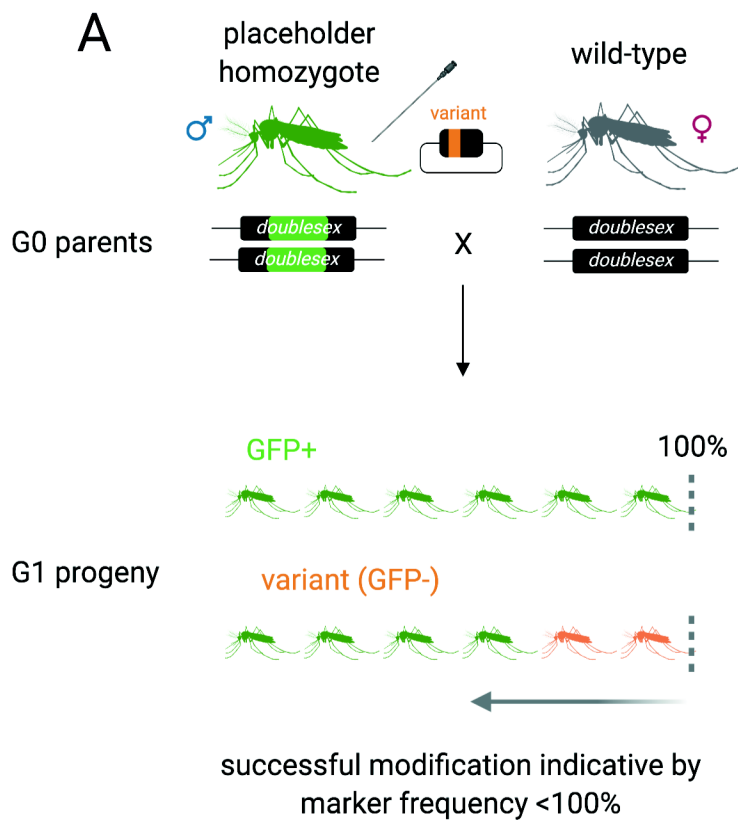


variants:

G->A SNP TTTATGTTTAAACACAGGTCAAGC**AGTGG**TCA

C->T SNP TTTATGTTTAAACACAGGTCAAG**TGGTGG**TCA

G->T SNP TTTATGTTTAAACACAGGTCA**ATCGGTGG**TCA





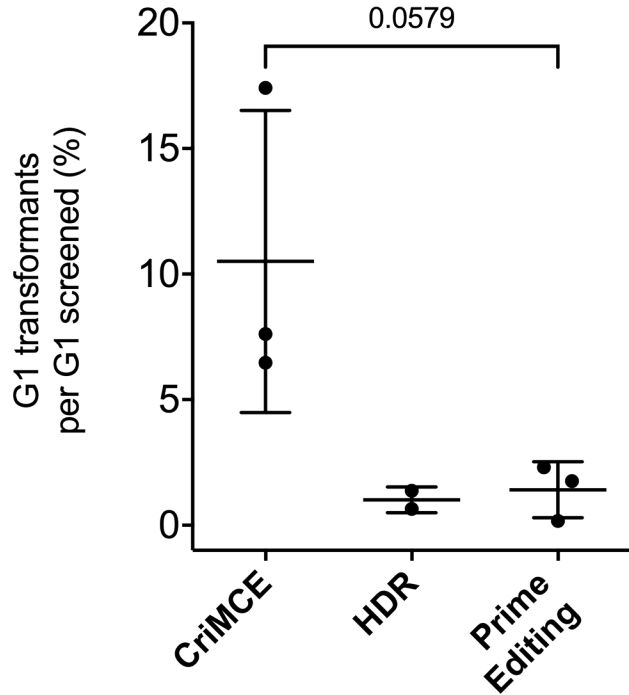
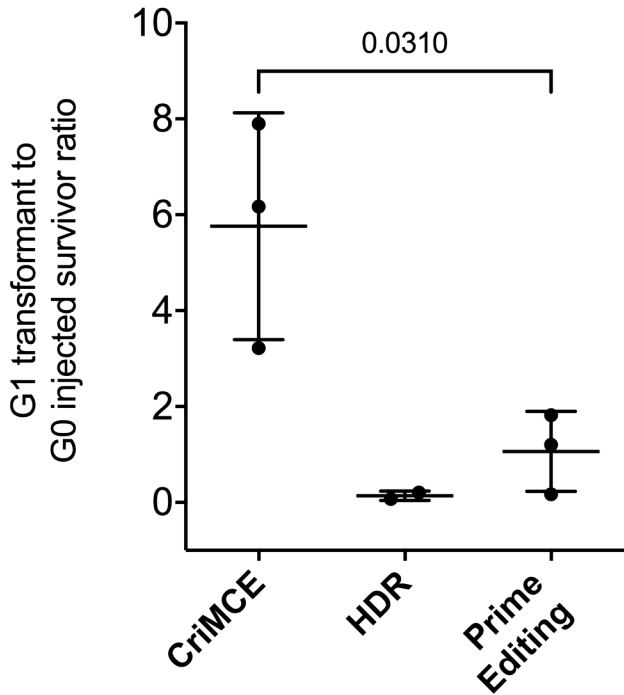


**Table 1. Comparison of CrimCE to different transgenesis methods for the introduction of small precise marker-less edits or marked transgenes.** Efficiency of each method is measured through the G1 transformant to G0 injected survivor ratio and the % of G1 transformants isolated from screened G1 progeny.

| Transgenesis method and study                              | Organism                          | Eggs injected N                | G0 Injected survivors N  | G1 transformants N | Total G1 screened N | G0 Founders N (%) | G1 transformant to G0 injected survivor ratio | G1 transformants per G1 screened % |       |       |
|--|-----------------------------------|--------------------------------|--------------------------|--------------------|---------------------|-------------------|---|------------------------------------|-------|-------|
| <b>Introduction of precise marker-less edit</b>            |                                   |                                |                          |                    |                     |                   |   |                                    |       |       |
| <b>CrimCE</b><br>present study                             | G->A                              | <i>Anopheles gambiae</i>       | 380                      | 18*<br>(59)        | 111 <sup>††</sup>   | 1716              | 7/18 (38.9)                                   | 6.17                               | 6.47  |       |
|  | C->T                              | <i>Anopheles gambiae</i>       | 1025                     | 21                 | 166 <sup>††</sup>   | 953               | 3/8 (37.5)                                    | 7.90                               | 17.42 |       |
|  | G->T                              | <i>Anopheles gambiae</i>       | 963                      | 23                 | 74 <sup>††</sup>    | 97                | 4/9 (44.4)                                    | 3.22                               | 7.62  |       |
| <b>HDR</b>   | Kistler et al. (2015)             | <i>Aedes aegypti</i>           | 636                      | 61 <sup>**</sup>   | 4 <sup>**</sup>     | 620               | N/A   | 0.07                               | 0.65  |       |
|  | Grigoraki et al. (2021)           | <i>Anopheles gambiae</i>       | 338                      | 19                 | 4 <sup>**</sup>     | 290               | 1/19 (5.0)                                    | 0.21                               | 1.38  |       |
| <b>Prime Editing</b><br>Bosch et al. (2021) <sup>***</sup> | Plasmid pegRNA                    | <i>Drosophila melanogaster</i> | 50                       | 18                 | 3 <sup>**</sup>     | 1767              | 1/18 (5.6)                                    | 0.17                               | 0.17  |       |
|  | Plasmid pegRNA+ sgRNA             | <i>Drosophila melanogaster</i> | 50                       | 15                 | 28 <sup>**</sup>    | 1594              | 6/15 (40.0)                                   | 1.20                               | 1.76  |       |
|  | Synthetic pegRNA                  | <i>Drosophila melanogaster</i> | 50                       | 11                 | 20 <sup>**</sup>    | 866               | 4/9 (44.4)                                    | 1.82                               | 2.31  |       |
| <b>Introduction of marked transgene</b>                    |                                   |                                |                          |                    |                     |                   |   |                                    |       |       |
| <b>RMCE</b><br>Hammond et al. (2016)                       | 7280                              | <i>Anopheles gambiae</i>       | 540                      | 56 <sup>**</sup>   | 15 <sup>†</sup>     | 4000              | N/A   | N/A                                | 0.38  |       |
|  | 11377                             | <i>Anopheles gambiae</i>       | 500                      | 21 <sup>**</sup>   | 4 <sup>†</sup>      | 2990              | N/A   | N/A                                | 0.13  |       |
|  | 5958                              | <i>Anopheles gambiae</i>       | 400                      | 49 <sup>**</sup>   | 2 <sup>†</sup>      | 4000              | N/A   | N/A                                | 0.05  |       |
| <b>HDR</b>   | Gratz et al. (2014)               | <i>Drosophila melanogaster</i> | N/A                      | 50                 | 599 <sup>†</sup>    | 7657              | 9/50 (18.0)                                   | 11.98                              | 7.82  |       |
|  | Gantz et al. (2015) <sup>††</sup> | <i>Anopheles stephensi</i>     | 680                      | 251 <sup>**</sup>  | 2 <sup>†</sup>      | 25,712            | N/A   | 0.01                               | 0.01  |       |
|  | Hammond et al. (2016)             | 7280                           | <i>Anopheles gambiae</i> | 350                | 48                  | 278 <sup>†</sup>  | 1536  | 9/48 (18.8)                        | 5.79  | 18.10 |
|  |                                   | 5958                           | <i>Anopheles gambiae</i> | 760                | 26                  | 51 <sup>†</sup>   | 3184  | 3/26 (11.5)                        | 1.96  | 1.60  |
|  | Adolfi et al. (2020)              | <i>Anopheles stephensi</i>     | 504                      | 184 <sup>**</sup>  | 96 <sup>†</sup>     | 25,293            | N/A   | 0.52                               | 0.38  |       |
|  | Ang et al. (2022)                 | 190-perfect                    | <i>Aedes aegypti</i>     | N/A                | 271 <sup>**</sup>   | 350               | 9,774   | 13/13 (100.0) <sup>o</sup>         | 1.29  | 3.6   |
|  |                                   | 64+234-perfect                 | <i>Aedes aegypti</i>     | N/A                | 355 <sup>**</sup>   | 207               | 22,158  | 8/17 (47.1) <sup>o</sup>           | 0.58  | 0.93  |

\*Only 18 out of 59 G0 injected survivors were kept and crossed to obtain G1 transgenics, due to Covid-19 restrictions in April 2020.

\*\*In most studies G0 injected survivors are not being distinguished from non-injected survivors through transient expression of a fluorescent marker. The Kistler et al. (2015), Gantz et al. (2015), Hammond et al. (2016), Adolfi et al. (2020) and Ang et al. (2022) studies did not use such a method to distinguish injected survivors, or used all injected survivors (whether or not they showed signs of injection) to obtain transgenics.

\*\*\*Showing the set of injections with greater success for each method of prime editing: (a) using pegRNA expressed from a plasmid to provide cleavage and a template for repair, (b) using plasmid pegRNA together with an sgRNA to provide cleavage, (c) injecting a synthetic pegRNA straight away.

<sup>†</sup>Identified visually.

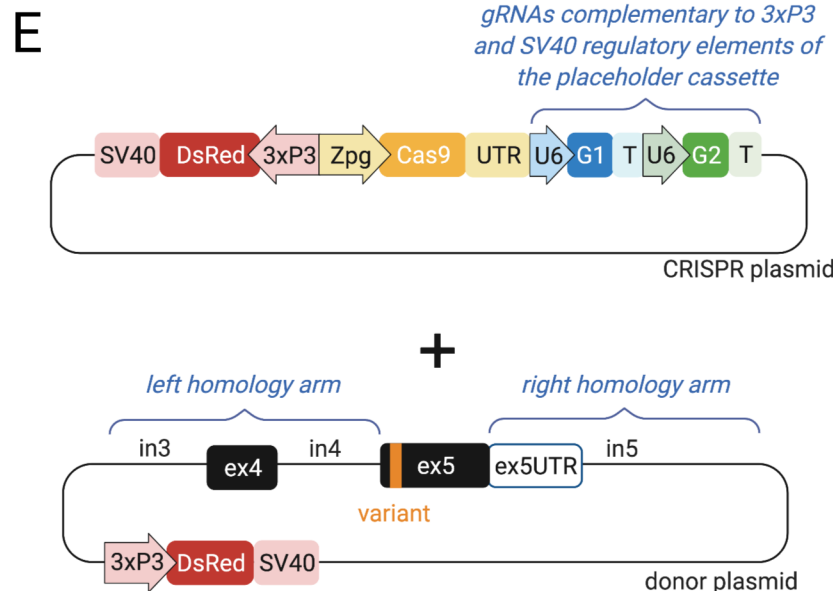
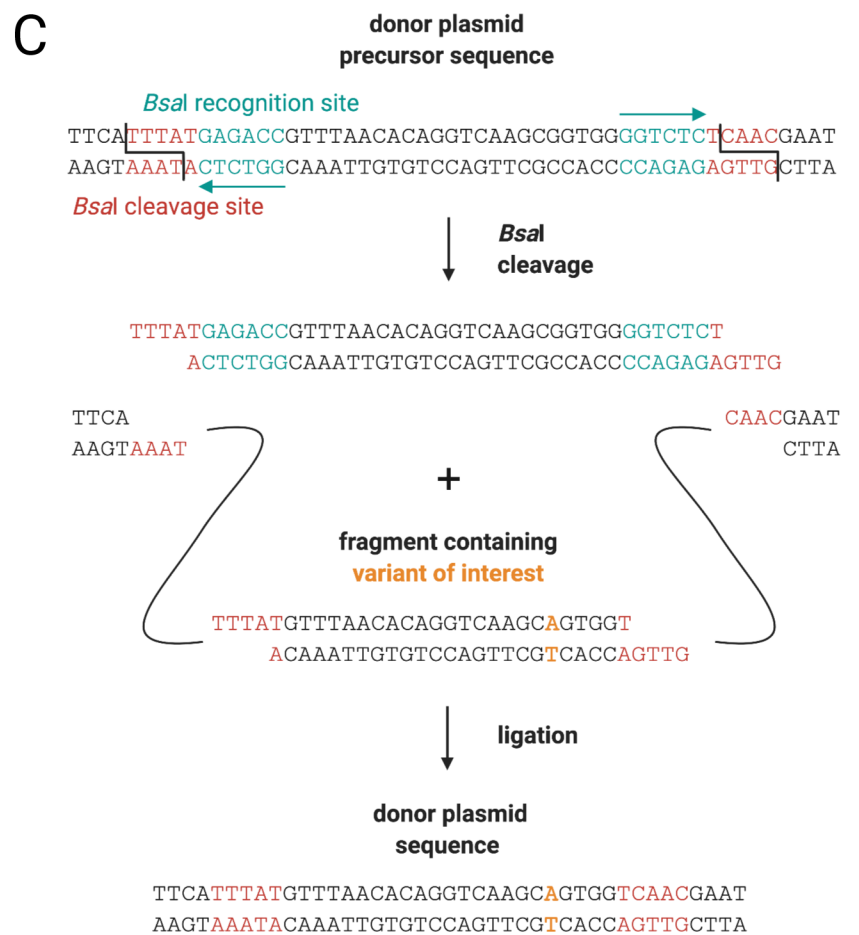
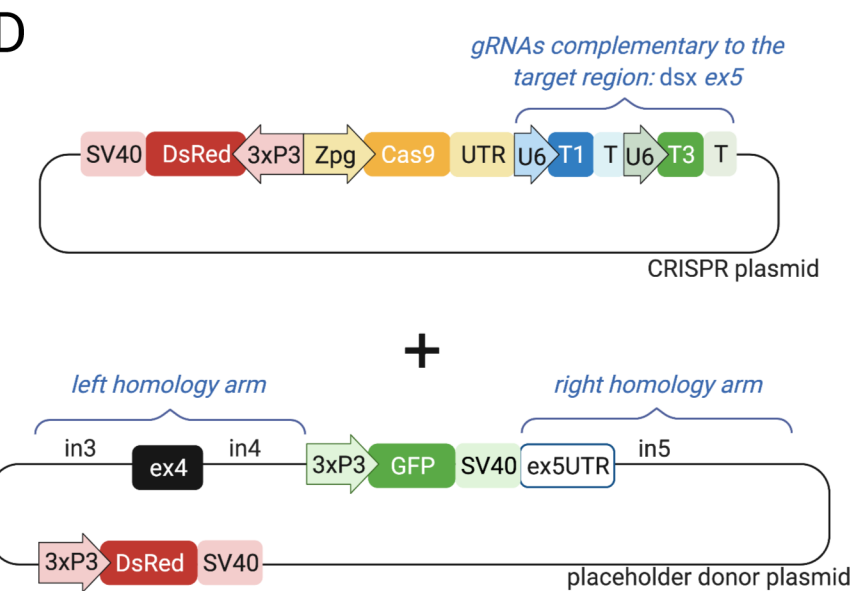
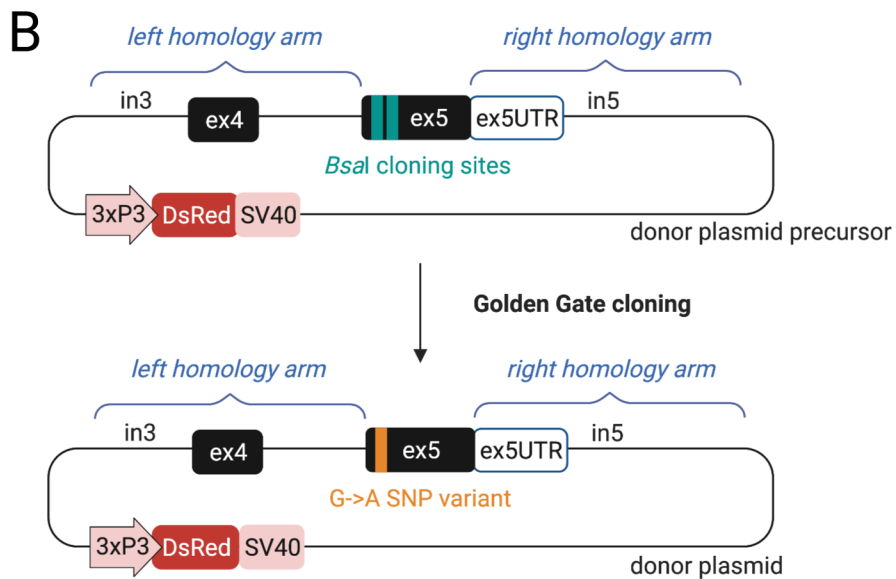
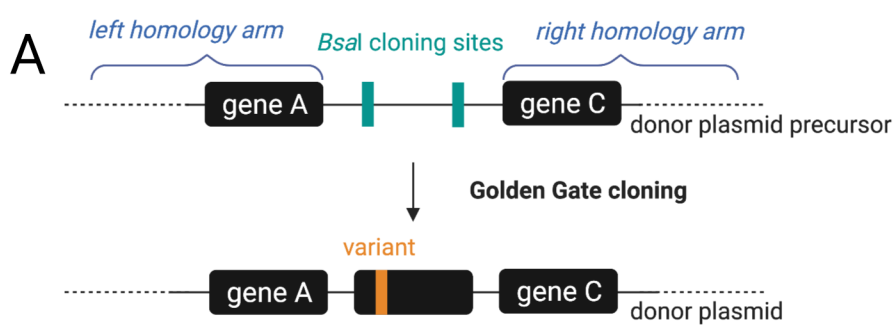
♦♦Identified through sequencing.

†The number of transformants is equal to the number of individuals lacking a fluorescent marker in the progeny of placeholder homozygotes. The number of transformant in the progeny of placeholder heterozygotes it was estimated using this formula:  $(\text{Total G1})/2 - \text{GFP}^+ - \text{RFP}^+$ .

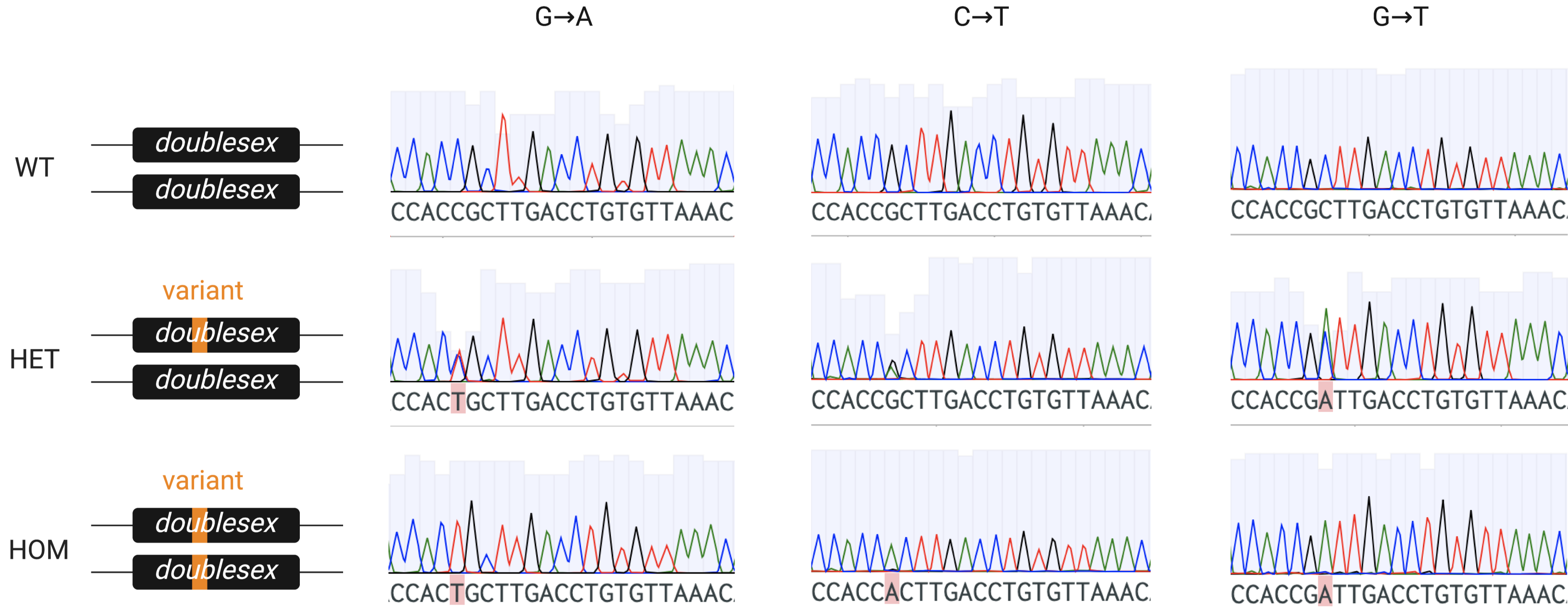
††Note that the transgene integrated by HDR in the Gantz et al. (2015) study was significantly larger in size compared to all other studies, which could have reduced efficiency of integration.

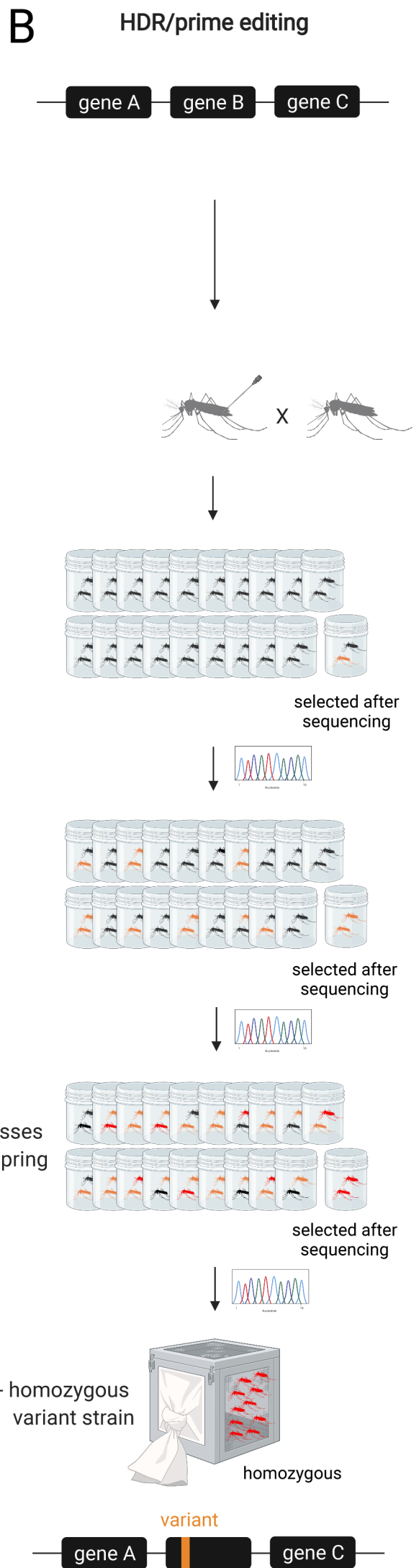
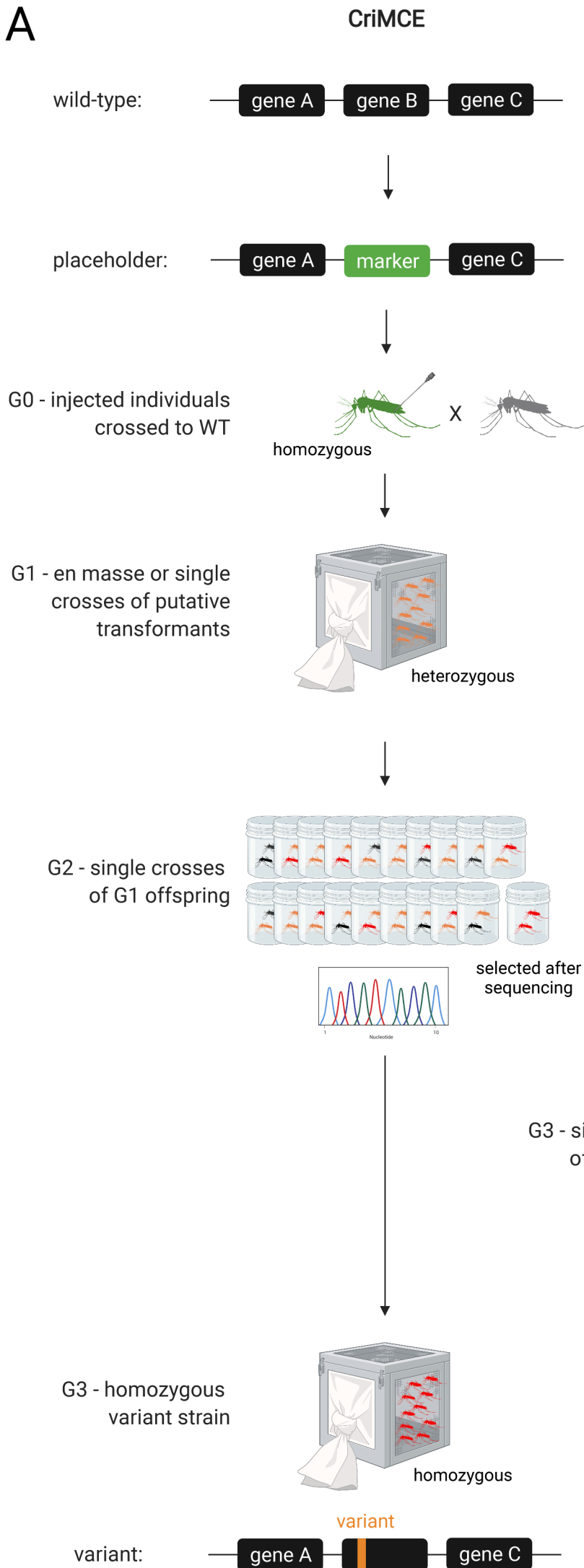
°The number of G0 founder pools that gave G1 transformants out of total G0 survivor pools is shown.

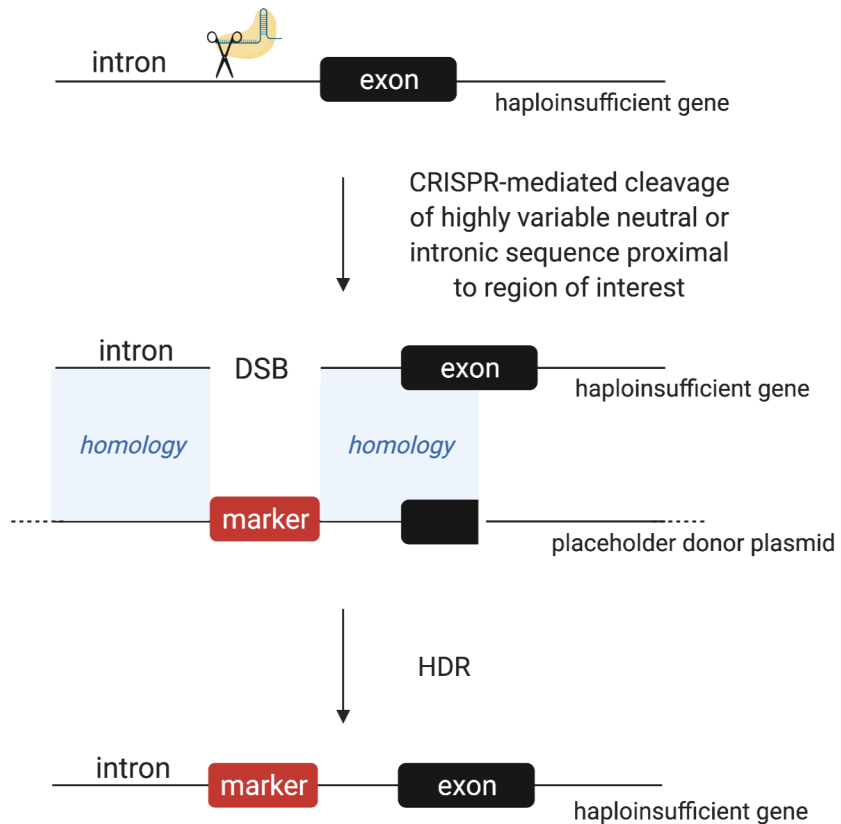
| Transgenesis method and study                   | Organism                | Eggs injected N                | G0 Injected survivors N  | G1 transformants N | Total G1 screened N | G0 Founders N (%) | G1 transformant to G0 injected survivor ratio | G1 transformants per G1 screened % |       |       |
|---|-------------------------|--------------------------------|--------------------------|--------------------|---------------------|-------------------|---|------------------------------------|-------|-------|
| <b>Introduction of precise marker-less edit</b> |                         |                                |                          |                    |                     |                   |   |                                    |       |       |
| CRISPR present study                            | G->A                    | <i>Anopheles gambiae</i>       | 380                      | 18* (59)           | 111*+               | 1716              | 7/18 (38.9)                                   | 6.17                               | 6.47  |       |
|   | C->T                    | <i>Anopheles gambiae</i>       | 1025                     | 21                 | 166*+               | 953               | 3/8 (37.5)                                    | 7.90                               | 17.42 |       |
|   | G->T                    | <i>Anopheles gambiae</i>       | 963                      | 23                 | 74*+                | 97                | 4/9 (44.4)                                    | 3.22                               | 7.62  |       |
| HDR   | Kistler et al. (2015)   | <i>Aedes aegypti</i>           | 636                      | 61**               | 4**                 | 620               | N/A   | 0.07                               | 0.65  |       |
|   | Grigoraki et al. (2021) | <i>Anopheles gambiae</i>       | 338                      | 19                 | 4**                 | 290               | 1/19 (5.0)                                    | 0.21                               | 1.38  |       |
| Prime Editing Bosch et al. (2021)***            | Plasmid pegRNA          | <i>Drosophila melanogaster</i> | 50                       | 18                 | 3**                 | 1767              | 1/18 (5.6)                                    | 0.17                               | 0.17  |       |
|   | Plasmid pegRNA+ sgRNA   | <i>Drosophila melanogaster</i> | 50                       | 15                 | 28**                | 1594              | 6/15 (40.0)                                   | 1.20                               | 1.76  |       |
|   | Synthetic pegRNA        | <i>Drosophila melanogaster</i> | 50                       | 11                 | 20**                | 866               | 4/9 (44.4)                                    | 1.82                               | 2.31  |       |
| <b>Introduction of marked transgene</b>         |                         |                                |                          |                    |                     |                   |   |                                    |       |       |
| RMCE Hammond et al. (2016)                      | 7280                    | <i>Anopheles gambiae</i>       | 540                      | 56**               | 15*                 | 4000              | N/A   | N/A                                | 0.38  |       |
|   | 11377                   | <i>Anopheles gambiae</i>       | 500                      | 21**               | 4*                  | 2990              | N/A   | N/A                                | 0.13  |       |
|   | 5958                    | <i>Anopheles gambiae</i>       | 400                      | 49**               | 2*                  | 4000              | N/A   | N/A                                | 0.05  |       |
| HDR   | Gratz et al. (2014)     | <i>Drosophila melanogaster</i> | N/A                      | 50                 | 599*                | 7657              | 9/50 (18.0)                                   | 11.98                              | 7.82  |       |
|   | Gantz et al. (2015)††   | <i>Anopheles stephensi</i>     | 680                      | 251**              | 2*                  | 25,712            | N/A   | 0.01                               | 0.01  |       |
|   | Hammond et al. (2016)   | 7280                           | <i>Anopheles gambiae</i> | 350                | 48                  | 278*              | 1536  | 9/48 (18.8)                        | 5.79  | 18.10 |
|   |                         | 5958                           | <i>Anopheles gambiae</i> | 760                | 26                  | 51*               | 3184  | 3/26 (11.5)                        | 1.96  | 1.60  |
|   | Adolfi et al. (2020)    | <i>Anopheles stephensi</i>     | 504                      | 184**              | 96*                 | 25,293            | N/A   | 0.52                               | 0.38  |       |
|   | Ang et al. (2022)       | 190-perfect                    | <i>Aedes aegypti</i>     | N/A                | 271**               | 350               | 9,774   | 13/13 (100.0)°                     | 1.29  | 3.6   |
| 64+234-perfect                                  |                         | <i>Aedes aegypti</i>           | N/A                      | 355**              | 207                 | 22,158            | 8/17 (47.1)°                                  | 0.58                               | 0.93  |       |



Reverse strand Sanger sequencing reads:





**A****B**